HHS Public Access

Author manuscript

Acta Biomater. Author manuscript; available in PMC 2018 September 01.

Published in final edited form as:

Acta Biomater. 2017 September 01; 59: 108–116. doi:10.1016/j.actbio.2017.06.033.

Peptide-Functionalized Poly[oligo(ethylene glycol) methacrylate] Brushes on Dopamine-Coated Stainless Steel for Controlled Cell Adhesion

Guillermo R. Alas[‡,1], **Rachit Agarwal**[‡,2], **David M. Collard**[1,*], and **Andrés J. García**[2,*]

[1]School of Chemistry and Biochemistry, Georgia Institute of Technology, Atlanta GA 30332

[2]Woodruff School of Mechanical Engineering and Petit Institute for Bioengineering and Bioscience, Georgia Institute of Technology, Atlanta, GA 30332

Abstract

The modification of the surface of surgical implants with cell adhesion ligands has emerged as a promising approach to improve biomaterial-host interactions. However, these approaches are limited by the non-specific adsorption of biomolecules and uncontrolled presentation of desired bioactive ligands on implant surfaces. This leads to sub-optimal integration with host tissue and delayed healing. Here we present a strategy to grow non-fouling polymer brushes of oligo(ethylene glycol) methacrylate by atom transfer radical polymerization from dopamine-functionalized clinical grade 316 stainless steel. These brushes prevent non-specific adsorption of proteins and attachment of cells. Subsequently, the brushes can be modified with covalently tethered adhesive peptides that provide controlled cell adhesion. This approach may therefore have broad application to promote bone growth and improvements in osseointegration.

Graphical Abstract

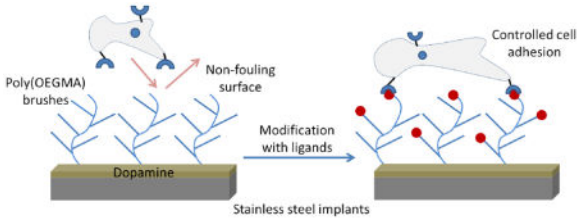

*Corresponding Authors: Prof. Andrés J. García, Woodruff School of Mechanical Engineering, Petit Institute for Bioengineering and Bioscience, Georgia Institute of Technology, Atlanta, GA 30332-0363 (USA), andres.garcia@me.gatech.edu. Prof. David M. Collard, School of Chemistry and Biochemistry, Georgia Institute of Technology, Atlanta, GA 30332-0400 (USA), david.collard@chemistry.gatech.edu.

‡Authors contributed equally

Conflict of interest

The authors declare no competing financial interest.

Keywords

surface modification; biomaterials; polymer brush; non-fouling surfaces; mesenchymal stem cells; RGD peptide

1. Introduction

Stainless steel (SS) is used widely in medical devices for bone, dental, and cardiovascular applications [1, 2]. Type 316 SS is attractive for orthopaedic applications such as fracture fixation by virtue of its high shear strength relative to that of other metals that are commonly used in such applications (e.g., titanium), along with its resistance to corrosion, cost effectiveness, and ease of manufacturing [1, 3]. However, SS implants are subject to relatively high rates of failure over long periods of time due to implant loosening, inflammation and bone resorption [4, 5]. For example, in osteoporotic fracture repairs, unstable fixation occurs in 5–23% of cases due to screw loosening and cutout [6–8]. Loosening rates of 18–27% have been reported for pedicle screws [9–11], and implant loosening results in pain, loss of spinal alignment and pseudoarthrosis. Various strategies have been explored to improve osseointegration of metal implants [12–17]. However, there is still a significant need to further improve performance.

Passive adsorption of cell adhesive proteins onto metallic implants provides biological coatings that promote osseointegration [18–20]. These proteins provide instructive cues to mediate cell attachment and differentiation [20–24]. However, passive adsorption of proteins onto the surface of the implant often leads to denaturation and loss of activity [25, 26]. Pre-adsorbed proteins can also be replaced by other proteins that have stronger affinity for the surface [27]. Therefore, significant efforts have centered on the development of stable coatings that prevent non-specific protein adsorption and which present selected ligands to promote adhesion and stimulate function of specific cells [28–31].

Self-assembled monolayers (SAMs) have long been explored to modify implant surfaces and thereby allow for control over protein adsorption and cell adhesion [28–33]. However, such coatings are often limited by the type of substrate. Most studies of SAMs have focused on gold and silver substrates, which are not ideal as implantable biomaterials. Another drawback of this approach is the limited resistance of SAMs to biofouling [28, 29]. In contrast, films consisting of polymer brushes on metallic substrates can provide stable, non-fouling coatings that do not elicit negative inflammatory responses [18, 34]. In “grafting to” approaches, pre-synthesized polymers are chemically attached to the surface. Whereas this has served as a successful strategy to attain control over protein adsorption and the attachment of cells, steric crowding between polymer chains limits the graft density and functionality [30, 35, 36]. On the other hand, “grafting from” approaches involve polymerization of monomers from an initiator that is bound to the substrate. The diffusion of small molecule monomers to the interface presents a low barrier for the preparation of dense polymer brushes. This strategy allows for the formation of dense films with control of the thickness by variation of polymerization conditions. Such “grafting from” polymerization of

oligo(ethylene glycol)-based monomers on titanium provides robust polymer brushes that resist protein adsorption and biofouling [35].

Controlled radical polymerizations such as atom transfer radical polymerization (ATRP) and reversible addition fragmentation chain transfer (RAFT) provide facile routes for the growth of polymer brushes on metallic substrates [30, 37–39]. Surface-initiated ATRP of oligo(ethylene glycol) methacrylate (OEGMA) provides a polymer brush that consists of a poly(methacrylate) backbone with pendant poly(ethylene glycol) (PEG) side chains. This provides the substrate with a robust hydrophilic coating that resists protein adsorption and cellular attachment [34]. The non-fouling properties of these brushes may be attributed to the presence of a high density of hydrated and dynamic PEG chains [40, 41].

Xiao *et al.* recently described a “grafting to” approach to attach functionalized PEG chains on to SS surfaces [42]. They demonstrated that this modification resulted in a decrease in platelet adhesion to the surface. However, the presence of residual levels of adherent platelets on the surfaces might be attributed to the inherently low-density of the brush formed by the “grafting to” approach. In addition, the lack of reactive functional groups on the grafted polymer chains limits the opportunity to decorate these surfaces with adhesive peptides that direct cell adhesion and signaling. Here, we present a modified approach to graft polymer brushes from medical-grade SS using surface-initiated ATRP to provide a non-biofouling surface. The strategy relies on the covalent attachment of an ATRP initiator to a layer of polydopamine on the substrate surface. We further show that these brushes can be modified with peptide ligands that control cell adhesion. These peptide-modified surfaces could improve the osseointegration of SS implants, such as screws and rods. The wide use of SS in biomedical devices suggests that this approach may be of broad applicability.

2. Materials and methods

2.1. Materials

Foils (100 mm × 100 mm) of 316 SS and 316L polished SS (Goodfellow, Pittsburgh, PA, USA) were cut into 10 mm × 10 mm coupons and a 0.8 mm hole was drilled in one corner. 316L SS 20-gauge wire was obtained from Beadlon (Valley Township, PA, USA). Oligo(ethylene glycol) methacrylate (OEGMA), Cu(I)Br, 2,2′-bipyridyl, ethyl 2-bromoisobutyrate, dopamine hydrochloride, anhydrous pyridine, hydrogen hexachloroplatinate (IV) hexahydrate, anhydrous dimethylformamide (DMF), 10-undecen-1-ol, dimethylchlorosilane, 1-ethyl-3-(3-*N,N*-dimethylaminopropyl)carbodiimide hydrochloride, 2-bromoisobutyryl bromide and *N*-hydroxysuccinimide (NHS) were purchased from Sigma-Aldrich (Milwaukee, WI, USA). Succinic anhydride was purchased from Alfa Aesar (Wardhill, MA, USA). For the polymerization of OEGMA, DI H_2O and methanol (MeOH) (VWR, Atlanta, GA, USA) were degassed by bubbling a stream of argon through the solvents for 3 h. Peptide ligands (RGD (GRGDSPC) or RDG (GRDGSPC) or RGD-FITC (GRGDSPK conjugated to fluorescein isothiocyanate(FITC))) were custom synthesized by GenScript (Piscataway, NJ, USA)

2.2. Preparation of polymer brush thin films

2.2.1. Preparation of SS surface—SS coupons were cleaned by soaking them for 1 min in H_2O and then acetone, and drying under a stream of N_2. The coupons were then placed in a ceramic slide holder and submerged into stirred piranha solution (3:1 conc. H_2SO_4:30% H_2O_2) for 1 h at room temperature. The coupons were soaked for 1 min in a large volume of H_2O twice, acetone twice, and for 10 seconds in methanol, 1 min in THF, and 1 min in hexane. They were then dried under a stream of N_2.

2.2.2. Deposition of dopamine layer on SS surface—Dopamine hydrochloride (91 mg, 0.47 mmol) was dissolved in a stirred solution of 10 mM Tris buffer (pH 8.5) at 60 °C. Freshly cleaned 316 SS coupons were suspended on a 316L SS wire and submerged into the heated solution of dopamine for 2 h. The suspended coupons were rinsed by immersion in MeOH (200 mL) for 10 min and DI H_2O (200 mL) for 10 min. The coupons were rinsed with MeOH for 10 sec, and immersed in THF (1 min) and hexane (1 min), and dried under a stream of N_2 immediately prior to attachment of the initiator.

2.2.3. Covalent attachment of initiator—An oven-dried glass reactor was subjected to three cycles of vacuum and back-filling with argon. Anhydrous pyridine (1.6 mL, 20 mmol) and anhydrous THF (80 mL) were placed in the reactor under a stream of argon. The reactor was cooled in an ice bath for 1 h, and the wire-suspended dopamine-modified SS coupons were immersed into the solvent. 2-Bromoisobutyryl bromide (2.4 mL, 19 mmol) was added slowly to the solvent with stirring. The reactor was removed from the ice bath and the mixture was vigorously stirred for 1 day to prevent precipitate from depositing onto the surface of the steel.

2.2.4. Deposition of poly(OEGMA) brush polymer on 316 SS—A flask containing a mixture of MeOH (40 mL) and DI water (10 mL) under argon was immersed in liquid nitrogen and subjected to three freeze-pump-thaw cycles (freezing the solution in liquid nitrogen for 15 min, applying vacuum for 20 min, and then thawing the solution in a warm water bath until the evolution of gas bubbles had ceased). The degassed solution was frozen in liquid nitrogen and CuBr (0.44 g, 3.7 mmol), OEGMA (24 mL, 44 mmol), and 2,2′-dipyridyl (0.96 g, 6.3 mmol) were added under a flow of argon. The reaction mixture was allowed to warm to room temperature. The polymerization solution was subjected to three additional freeze-pump-thaw cycles. Cooling was performed step-wise, with cooling in an ice-cold water followed by an acetone-dry ice bath for 15 min prior to cooling in liquid nitrogen. This prevents the violent release of dissolved gas upon application of vacuum. Initiator-modified 316 SS coupons were suspended from a wire which was then mounted in a Soxhlet extraction thimble. This was placed atop the frozen polymerization solution under a strong flow of argon. The reactor was closed and subjected to three cycles of vacuum and back-filling with argon. The cooling bath was removed and the polymerization mixture was allowed to thaw. The Soxhlet extractor thimble was lowered into the solution, thereby filtering out undissolved solids (which deposit on the SS substrates in the absence of the thimble). The vessel was placed on a platform rocker and polymerization was allowed to proceed for 20 h. The coupons were removed from the polymerization mixture and

immersed in MeOH for 15 min, dried under a stream of N_2 gas and immersed in a sealed container of PBS for storage.

2.2.5. Characterization of poly(OEGMA) films—The polymer brush thin films were characterized by X-ray photon spectroscopy (XPS), water contact angle measurements, and ellipsometry. XPS spectra were recorded on a Surface Science Instruments S-probe spectrometer at the Surface Analysis Center for Biomedical Problems (NESAC/BIO), Seattle, WA, USA. Surfaces were tested for hydrophilicity by water contact measurements using a contact angle goniometer under ambient conditions (Ramé-Hart, Succasunna, New Jersey, USA). Ellipsometry measurements were performed using a Sopra GES5 variable angle spectroscopic ellipsometer (Sopra Inc., Palo Alto, CA) and the accompanying GESPack software package for data analysis. Samples were placed in DI water and scanned from 1.5 eV to 6.0 eV at 0.05 eV intervals using an incident angle of 70°. The thickness of all layers on each surface was determined using the regression method in Sopra's Winelli software (version 4.08).

2.3. Peptide coupling to poly(OEGMA) surfaces

2.3.1 Treatment of poly(OEGMA) side chain termini with succinic anhydride—Poly(OEGMA) brush-modified SS coupons were removed from PBS and soaked in MeOH for 10 sec, in THF for 1 min and in hexane for 1 min, and dried under a flow of argon. The coupons were mounted in an oven-dried ceramic holder that was placed in a solution of succinic anhydride (1.6 g, 16 mmol) in anhydrous DMF (60 mL) in an oven-dried, argon-purged jointed glass vessel. The mixture was heated to 60 °C under argon for 4 h. The coupons were then removed from the reaction mixture, rinsed twice with DMF, and immersed of DI H_2O for 5 min and in fresh DI H_2O for an additional 1 min. The coupons were stored in PBS.

2.3.2 Peptide conjugation—Succinic anhydride-modified poly(OEGMA) coupons were immersed in 1 mL of 0.1 M MES buffer (pH 5.5) solution containing 2 mM 1-ethyl-3-(3-*N,N*-dimethylaminopropyl)carbodiimide hydrochloride and 5 mM *N*-hydroxysuccinimide for 30 min at room temperature. The coupons were washed with PBS and immediately incubated in solutions of peptide for 2 h (100 μg/mL RGD, RDG or RGD-FITC in PBS, pH 7.4). Peptide-treated surfaces were then incubated in 20 mM glycine for 4 h to quench any unreacted active esters. The coupons were rinsed with PBS and stored in PBS.

2.3.3 Quantification of peptide coupling on succinic modified brushes—A standard curve was prepared by drying known quantities (0 to 5 nmol) of FITC-RGD on SS coupons and imaging using a Nikon Eclipse E400 fluorescent microscope. Three images were taken for each coupon and analyzed for average fluorescence using ImageJ (NIH, Bethesda, MD, USA). RGD-FITC reacted brushes were then similarly imaged and the amount of immobilized peptide was determined by comparison to the standard curve.

2.4. Analysis of protein adsorption

To test the non-fouling nature of modified SS surfaces, protein adsorption assays were performed using donkey anti-mouse IgG antibody conjugated to alkaline phosphatase (ALP)

(Jackson Immunoresearch, West Groove, PA, USA) and human plasma fibronectin (Life Technologies, Carlsbad, CA, USA). Unmodified and modified coupons were incubated with 1.0 μg/mL of protein in PBS for 30 min and then extensively washed with PBS containing 0.05 % (v/v) Triton-X-100. For ALP-conjugated IgG, samples were incubated with 5-methyl umbelliferyl phosphate substrate (60 mg/mL) for 20 min at room temperature and fluorescence was determined at excitation/emission of 360 nm/465 nm on a HTS 7000 Plus plate reader (Perkin Elmer, Akron, Ohio, USA). For fibronectin, samples were incubated in 1% w/v casein blocker (Life Technologies) and probed in a modified immunoassay using 1 mg/mL HFN7.1 antibody (Developmental Hybridoma Studies Bank, Iowa City, Iowa, USA). After several washes in buffer, the coupons were incubated in (ALP)-conjugated antibody (1 μg/mL in PBS) for 30 min. The coupons were washed with PBS buffer containing 0.05% Triton-x-100 and incubated with 5-methyl umbelliferyl phosphate substrate (60 mg/mL) for 20 min at room temperature prior to determination of fluorescence intensity.

SS 316 grade screws (McMaster Carr, Atlanta, GA, USA) (2.0 mm in thread length, 1.52 mm thread diameter) were used as a substrate for synthesis of brush polymer. Using a 1.5 mm diameter drill bit, a hole was made in an explanted rat tibia. Untreated and OEGMA screw implants were screwed into the hole. Screws were removed and then tested for protein adsorption as described above.

2.5. Analysis of cell adhesion

Poly(OEGMA)-SS coupons were rinsed with PBS, sterilized by brief immersion in 70% ethanol, rinsed with PBS, and incubated in PBS overnight at 37 °C to hydrate the poly(OEGMA) surface. Human mesenchymal stem cells (hMSCs) were obtained from the Institute of Regenerative Medicine at Texas A&M (College Station, TX, USA), cultured in Lonza mesenchymal stem cell medium (MSCM), and passaged every 3 to 4 days. Each coupon was seeded with 10,000 hMSCs in a separate well in a 24 well plate. Cells were allowed to adhere for 18 h at 37 °C and 5% CO_2. After 18 h, the coupons were washed with PBS, stained with Calcein-AM (1 μg/mL, Life Technologies) and imaged using a Nikon Eclipse E400 fluorescent microscope. Five images were taken for each coupon and analyzed for cell density and cell spreading area using ImageJ.

2.6. Analysis of cell proliferation

Each coupon was seeded with 10,000 hMSCs in a separate well in a 24-well plate. Cells were seeded in serum-containing media and allowed to adhere for 18 h at 37 °C and 5% CO_2. Proliferation was measured using the Click-iT® EdU AlexaFluor® 488 Imaging Kit (Life Technologies). Cells were incubated in EdU for 18 h, stained with Hoechst 33342 and imaged using a Nikon Eclipse E400 fluorescent microscope. Three images were taken for each coupon and analyzed for number of proliferating cells (AlexaFluor 488) and total number of nucleus (Hoechst 33342) using ImageJ.

2.7. Statistics

All data is presented as a mean with the standard deviation. Results were analyzed by two-tailed Student’s t-test or one-way ANOVA followed by Tukey’s multiple comparisons in

GraphPad Prism software. A confidence level of 95% was considered significant. All assays were conducted at least in triplicate.

3. Results

3.1. Deposition of poly(OEGMA) brushes on SS

We used a thin film of polydopamine as a foundation to attach an ATRP initiator to the SS substrate [43–47]. This strategy is illustrated in Figure 1. Immersion of cleaned SS substrates in a heated aqueous solution of dopamine results in the deposition of a red-brown layer of polydopamine. This resulted in a hydrophilic surface, as determined by water contact angle measurements (Table 1). The coupons were then immersed in a solution of 2-bromoisobutyryl bromide and pyridine in THF to covalently attach the ATRP initiator to the dopamine layer. The successful attachment of the 2-bromoisobutyryl group was confirmed by a dramatic increase in the water contact angle (Table 1) and through the presence of a bromine signal in the XPS spectra (Figure 2C, Table 2).

The initiator-modified SS surfaces were placed inside a cellulose Soxhlet extraction thimble and immersed in a solution of OEGMA, CuBr, 2,2′-bipyridyl in a 4:1 mixture of methanol and water. The extraction thimble serves to filter the reaction mixture to prevent excess insoluble CuBr from depositing onto the metal surfaces while allowing the soluble 2,2′-bipyridyl copper complex to catalyze formation of the polymer brush. Non-fouling surfaces were obtained only when the thimble was used to filter the polymerization mixture. Attempts to conduct the polymerization in the absence of the thimble resulted in the deposition of CuBr on the coupons and surfaces that were not non-fouling. The deposition of cell-resistant poly(OEGMA) polymer brushes also required stringent removal of oxygen from the polymerization reaction vessel.

3.2 Characterization of poly(OEGMA) brushes

The composition of the film deposited on the SS coupons, after deposition of polydopamine, modification with 2-bromoisobutyryl bromide, and polymerization of OEMGA, was analyzed using measurement of water contact angle, ellipsometry and XPS. XPS spectra of unmodified coupons show the expected peaks for SS, including peaks for nickel, iron, chromium, oxygen and carbon (Figure 2, Table 2). The addition of the dopamine layer was evident from a decrease of the signals from the SS substrate and the appearance of a new signal corresponding to nitrogen. Upon treatment of the dopamine-modified SS coupons with 2-bromoisobutyryl bromide, the XPS spectra showed the presence of a peak for bromine at 68.7 eV. After surface-initiated ATRP of OEGMA, the XPS spectra of the coupons only showed the expected peaks for carbon and oxygen of the polymer brushes. This is consistent with the formation of a relatively thick layer of poly(OEGMA) that fully attenuates the signal from the metallic substrate.

A high resolution scan was performed for the C1*s* region of the spectrum to evaluate the chemical composition of the polymer brush. The integration of the peaks in this region of the spectrum (C-C, 17.4%; C-O, 76.3%; and O-C=O, 6.3%) is in good agreement with the theoretical values that are expected for poly(OEGMA) (Figure 3, Table 3). For the analysis

of initiator attachment, a C=O peak is observed from the oxidation of catechol portion of polydopamine into the quinone form (not shown) [48]. Ellipsometric analysis of hydrated surfaces indicated a thickness of 122 ± 26 nm for the dopamine anchoring sublayer and 107 ± 13 nm for poly(OEGMA) coating. This thickness of poly(OEGMA) is well above the value of 10 nm that has previously been reported as necessary for anti-fouling behavior [30, 49].

3.3 Polymer brushes prevent protein adsorption onto SS

Protein adsorption assays were performed to examine the non-fouling nature of the polymer brush-modified SS coupons. The coupons were incubated in a solution of ALP-conjugated IgG or human fibronectin and assayed for adsorption of protein. These assays show a significant reduction in the adsorption of both proteins to the poly(OEGMA) brush-grafted SS compared to untreated SS ($p<0.001$) (Figure 4). This result demonstrates that the poly(OEGMA) brush coating significantly reduces non-specific protein adsorption compared to unmodified SS.

To examine the mechanical stability of the grafted brushes, brush-coated SS screws were inserted into cadaveric bone, removed, and then tested for resistance to protein adsorption by ELISA. As shown in Figure S1, such screws retained their non-fouling properties indicating that the polydopamine/poly(OEGMA) coating is strongly attached and stable to the mechanical load experienced during insertion.

3.4 Polymer brushes prevent cell attachment on SS

Cell adhesion assays were performed using human mesenchymal stem cells (hMSCs) in the presence of serum. Serum contains proteins such as fibronectin and vitronectin which typically adsorb onto surfaces and mediate cell adhesion [50]. Since poly(OEGMA) brush-grafted surfaces resist protein adsorption, our expectation was that these surfaces would not support cell attachment or spreading. hMSCs were cultured for 18 h on SS surfaces. Samples were rinsed and then stained with Calcein-AM for fluorescence imaging of adherent cells. As shown in Figure 5A–B, poly(OEGMA) surfaces displayed a significant reduction (>95% decrease) in the density of adherent cells compared to unmodified SS ($p < 0.001$) (Figure 5C). Cell spreading was also significantly reduced on poly(OEGMA)-modified substrates compared to unmodified SS (~60% decrease in surface area; $p < 0.03$) (Figure 5D). Reduction in cell density and spreading compared to untreated SS was not observed on dopamine and initiator-modified surfaces, indicating that the polymer brush is essential to prevent cell adhesion.

3.5 Modification of the polymer brush with adhesive ligands restores cell adhesion

Having demonstrated the cell adhesion-resistant nature of poly(OEGMA) brushes on SS, we evaluated whether the brushes could be functionalized with adhesive peptide ligands so as to direct cell adhesion. We focused on the immobilization of a short synthetic peptide that contains the arginine-glycine-aspartic acid (RGD) binding motif of the adhesive protein fibronectin. As a negative control, we used a peptide that contains the scrambled RDG sequence that does not support cell adhesion. The poly(OEGMA)-modified SS coupons were treated with succinic anhydride [51] to provide carboxylic acid groups at the termini of

the pendant PEG chains (Figure 6A). Whereas the use of base to promote the ring-opening of succinic anhydride has been reported for other PEG-containing brush polymers [52, 53], our attempts to use base to modify the dopamine-anchored poly(OEGMA) brush polymer films resulted in loss of non-fouling properties (supplementary methods, Figure S2). This might be explained by the previous observation that polydopamine is subject to degradation in the presence of base [43], or, by the base promoted hydrolysis of the ester linkages between the PEG side chains and the methacrylate backbone. Accordingly, we performed the ring-opening reaction of succinic anhydride on the poly(OEGMA)-bearing SS coupons in the absence of base.

The carboxyl acid groups of succinic anhydride-treated poly(OEGMA) films underwent reaction with *N*-hydroxysuccinimide (NHS) in the presence of 1-ethyl-3-(3-*N,N*-dimethylaminopropyl)carbodiimide hydrochloride (EDC) to provide active NHS-esters prior to exposure to peptides. XPS was performed on RGD-modified surfaces to detect the nitrogen signal associated with the peptide. However, no nitrogen signal was detected, mostly likely due to the low density of peptide on the surface. A surface density of 2.0 nmol/cm^2 of tethered ligands was determined by using a fluorescently-labeled RGD peptide.

hMSCs were cultured on RGD- and RDG-modified poly(OEGMA) surfaces for 18 h in serum-containing media. As shown in Figure 6B–E, RDG-modified brushes showed minimal cell adhesion and spreading, whereas RGD-conjugated brushes supported significantly higher cell adhesion and spreading. This result shows that cell attachment was specific to the RGD peptide and that these surfaces supported cell adhesion and spreading. Furthermore, we tested the ability of cells to proliferate on RGD-modified surfaces. Analysis of substrates after incubation with cells indicated that the RGD-modified polymer brushes support hMSC proliferation (Figure S3). As expected, RGD-modified surfaces supported lower cell densities compared to untreated SS. In this study, we focused on linear RGD peptide as a model peptide. We performed additional experiments with a cyclic RGD that has higher affinity for cell adhesion [54] and showed high cell densities on peptide-modified OEGMA surface (Figure S4).

4. Discussion

Passive adsorption of cell adhesive proteins onto metallic implants improves osseointegration [18, 19, 55, 56]. Although promising, such strategies have resulted in limited improvements due to uncontrolled presentation of ligands on the implant interface, denaturation of adhesive proteins, and displacement of physisorbed adhesive proteins by other molecules that have a strong binding affinity for the surface [25–27]. We hypothesized that controlled and stable presentation of adhesive peptides from SS surfaces, on a cell-resistant background, would lead to reduced non-specific protein adsorption and directed cell adhesion. We have previously demonstrated a significant level of control over the presentation of biomolecules on thin films of poly(OMEGA) brushes on titanium that were deposited on a monolayer of silane-bound initiator [35]. Such controlled presentation of cell adhesive ligands resulted in functional improvement for bone implants *in vivo* [18, 57]. However, our attempts to translate the polymerization of OEGMA on monolayers of silane–bound initiator to SS failed to produce non-fouling surfaces (see supplemental methods and

Figures S5, S6). This motivated us to change the surface modification strategy to use a foundation layer of polydopamine to attach an ATRP initiator for the controlled surface polymerization of OEGMA.

Dopamine has previously been used as a foundation coating layer for the formation of a brush polymer via ATRP [43–46]. Lee *et al.* showed that dopamine polymerizes to form thin films on a wide range of inorganic and organic substrates [43]. Reaction of the primary amines of the polydopamine surface can be performed to further modify the surface [43]. For example, Sin *et al.* have prepared non-fouling SS by deposition of a zwitterionic poly(sulfobetaine methacrylate) brush polymer on a polydopamine layer [47]. While this brush polymer prevented biofouling, it lacked functionality for the attachment of biological ligands or to provide additional functionality. Others have employed the approach of layering polydopamine on substrates to deposit polymer brushes on nylon, polyethylene terephthalate, and aluminum oxide surfaces [44–46].

We used a “grafting from” approach to deposit non-fouling polymer brushes whereby a polydopamine coating on SS was modified with an ATPR initiator to promote the polymerization of OEGMA (Figure 1). The kinetics for polymer growth by ATRP are governed by the interchange between the inactivated bromine-substituted form of the terminal methacrylate unit and the active copper complexed chain end. This results in a uniform and controlled growth of the poly(OEGMA) brush [58]. Indication that polymerization had occurred comes from surface analysis using XPS and ellipsometry (Figures 2 and 3). While ATRP provides a robust method for providing brush polymers, it does not allow for the characterization of molecular weight or grafting density. Sacrificial initiator has been previously used to characterize the molecular weight of surface bound brush polymers [59–61]. However, adding a sacrificial initiator and using the bulk polymerization as an indication of the degree of polymerization on the surface would alter the polymer growth on substrate. Nevertheless, the surface characterization, peptide density, and reproducible antifouling properties presented indicate high quality brush polymer of sufficient thickness and density.

The deposition of poly(OEGMA) brushes on SS resulted in surfaces that resist protein adsorption (Figure 4). Cell adhesion experiments with hMSCs also showed minimal cell attachment on poly(OEGMA) surfaces compared to untreated SS (Figure 5). An important aspect of this study was the ability to modify the non-fouling polymer brushes with adhesive ligands which could then be used to control cell adhesion. The ability to graft to the terminal ends of the brush polymer on stainless steel is an attractive technology as it allows for enhance customization for the attachment of a wide range of biological ligands. Polymer brushes were treated with succinic anhydride to impart the surface with carboxylic acid groups. These are subject to routine carbodiimide coupling with peptides. Polymer brushes modified in this manner with integrin ligands (RGD) demonstrated cell adhesion and spreading (Figure 6). We present this as a proof-of-concept for the promotion of cell adhesion and activities on SS substrates through the well-defined presentation of adhesive ligands on a substrate that has been modified to prevent non-specific protein adsorption. RGD, which binds to several receptors on cell surface [50], has wide application in

promoting bone formation on implant surfaces [21]. This approach might also be extended to other peptides (e.g., GFOGER) that display specific integrin signaling [19].

The methods described here provide a reproducible strategy to produce thick polymer brushes that prevent fouling with proteins and cells and also provide a method to allow for the facile coupling of biologically relevant ligands. Adhesive ligand-modified polymer brushes support cell adhesion and proliferation while still maintaining the non-fouling properties of the brush. Surfaces modified with scrambled peptide sequences (e.g., RDG) do not support cell adhesion.

5. Conclusions

We have presented a robust approach to modify medical grade stainless steel with poly(OEGMA) brushes that prevent protein adsorption and cell adhesion. This strategy is amenable to modification of complex geometries of implants such as screws, pins and stents, which are challenging to functionalize using dry anisotropic approaches such as vapor deposition. The poly(OEGMA) brushes significantly reduce protein adsorption and cell adhesion compared to the unmodified substrate surface. While preventing the passive adsorption of proteins, the brushes also allow for controlled tethering of bioactive peptide ligands to provide for control of cell adhesion. The approach may therefore have broad application to improve osseointegration and promote bone growth and regeneration on stainless steel implants in surgical bone repair.

Supplementary Material

Refer to Web version on PubMed Central for supplementary material.

Acknowledgments

This work was funded by NIH grant R01 AR062920. hMSCs were provided by the Texas A&M Health Science Center College of Medicine Institute for Regenerative Medicine at Scott & White through a grant from ORIP of the NIH grant P40 OD011050. The surface analysis experiments (XPS) done at the National ESCA and Surface Analysis Center for Biomedical Problems (NESAC/BIO), Seattle, WA, USA were supported by National Institute for Biomedical Imaging and Bioengineering (NIBIB) grant P41 EB002027. We acknowledge the contributions of Prof. Robert Latour and Dr. Gulya Korneva for the ellipsometry analyses of the surface layers presented in this paper. These analyses were conducted under the Bioengineering and Bioimaging Core of the SC BioCraft Research Center at Clemson University supported by an Institutional Development Award (IDeA) from the National Institute of General Medical Sciences of NIH under grant number P20GM103444.

References

1. Disegi JA, Eschbach L. Stainless steel in bone surgery. Injury. 2000; 31(Suppl 4):2–6.
2. O'Brien B, Carroll W. The evolution of cardiovascular stent materials and surfaces in response to clinical drivers: A review. Acta Biomater. 2009; 5:945–958. [PubMed: 19111513]
3. Muller R, Abke J, Schnell E, Macionczyk F, Gbureck U, Mehrl R, Ruszczak Z, Kujat R, Englert C, Nerlich M, Angele P. Surface engineering of stainless steel materials by covalent collagen immobilization to improve implant biocompatibility. Biomaterials. 2005; 26:6962–72. [PubMed: 15967497]
4. Abu-Amer Y, Darwech I, Clohisy J. Aseptic loosening of total joint replacements: mechanisms underlying osteolysis and potential therapies. Arthritis Res Ther. 2007; 9(Suppl 1):1–7.

5. Bauer TW, Schils J. The pathology of total joint arthroplasty. Skeletal Radiol. 1999; 28:423–432. [PubMed: 10486010]
6. Stromsoe K. Fracture fixation problems in osteoporosis. Injury. 2004; 35:107–13. [PubMed: 14736465]
7. Lindner T, Kanakaris NK, Marx B, Cockbain A, Kontakis G, Giannoudis PV. Fractures of the hip and osteoporosis: the role of bone substitutes. J Bone Joint Surg Br. 2009; 91:294–303. [PubMed: 19258602]
8. Moroni A, Hoang-Kim A, Lio V, Giannini S. Current augmentation fixation techniques for the osteoporotic patient. Scand J Surg. 2006; 95:103–109. [PubMed: 16821653]
9. Pihlajamaki H, Myllynen P, Bostman O. Complications of transpedicular lumbosacral fixation for non-traumatic disorders. J Bone Joint Surg Br. 1997; 79:183–9. [PubMed: 9119839]
10. Soini J, Laine T, Pohjolainen T, Hurri H, Alaranta H. Spondylodesis augmented by transpedicular fixation in the treatment of olisthetic and degenerative conditions of the lumbar spine. Clin Orthop Relat Res. 1993; 297:111–6.
11. Ohlin A, Karlsson M, Duppe H, Hasserius R, Redlund-Johnell I. Complications after transpedicular stabilization of the spine. A survivorship analysis of 163 cases. Spine. 1994; 19:2774–9. [PubMed: 7899978]
12. Boyan BD, Sylvia VL, Liu Y, Sagun R, Cochran DL, Lohmann CH, Dean DD, Schwartz Z. Surface roughness mediates its effects on osteoblasts via protein kinase A and phospholipase A2. Biomaterials. 1999; 20:2305–2310. [PubMed: 10614936]
13. Klokkevold PR, Johnson P, Dadgostari S, Davies JE, Caputo A, Nishimura RD. Early endosseous integration enhanced by dual acid etching of titanium: a torque removal study in the rabbit. Clin Oral Implants Res. 2001; 12:350–357. [PubMed: 11488864]
14. Wennerberg A, Albrektsson T. Suggested guidelines for the topographic evaluation of implant surfaces. Int J Oral Maxillofac Implants. 2000; 15:331–44. [PubMed: 10874798]
15. Soballe K. Hydroxyapatite ceramic coating for bone implant fixation. Mechanical and histological studies in dogs. Acta Orthop Scand Suppl. 1993; 255:1–58. [PubMed: 8237337]
16. Cook SD, Thomas KA, Dalton JE, Volkman TK, Whitecloud TS 3rd, Kay JF. Hydroxylapatite coating of porous implants improves bone ingrowth and interface attachment strength. J Biomed Mater Res. 1992; 26:989–1001. [PubMed: 1429760]
17. Agarwal R, Garcia AJ. Biomaterial strategies for engineering implants for enhanced osseointegration and bone repair. Adv Drug Deliv Rev. 2015; 94:53–62. [PubMed: 25861724]
18. Petrie TA, Raynor JE, Reyes CD, Burns KL, Collard DM, Garcia AJ. The effect of integrin-specific bioactive coatings on tissue healing and implant osseointegration. Biomaterials. 2008; 29:2849–57. [PubMed: 18406458]
19. Wojtowicz AM, Shekaran A, Oest ME, Dupont KM, Templeman KL, Hutmacher DW, Guldberg RE, Garcia AJ. Coating of biomaterial scaffolds with the collagen-mimetic peptide GFOGER for bone defect repair. Biomaterials. 2010; 31:2574–82. [PubMed: 20056517]
20. Agarwal R, González-García C, Torstrick B, Guldberg RE, Salmerón-Sánchez M, García AJ. Simple coating with fibronectin fragment enhances stainless steel screw osseointegration in healthy and osteoporotic rats. Biomaterials. 2015; 63:137–145. [PubMed: 26100343]
21. Ferris DM, Moodie GD, Dimond PM, Giorani CWD, Ehrlich MG, Valentini RF. RGD-coated titanium implants stimulate increased bone formation in vivo. Biomaterials. 1999; 20:2323–2331. [PubMed: 10614938]
22. Reyes CD, Garcia AJ. Engineering integrin-specific surfaces with a triple-helical collagen-mimetic peptide. J Biomed Mater Res A. 2003; 65:511–23. [PubMed: 12761842]
23. Reyes CD, Petrie TA, Burns KL, Schwartz Z, Garcia AJ. Biomolecular surface coating to enhance orthopaedic tissue healing and integration. Biomaterials. 2007; 28:3228–35. [PubMed: 17448533]
24. Marie PJ. Targeting integrins to promote bone formation and repair. Nat Rev Endocrinol. 2013; 9:288–95. [PubMed: 23358353]
25. Kashiwagi K, Tsuji T, Shiba K. Directional BMP-2 for functionalization of titanium surfaces. Biomaterials. 2009; 30:1166–75. [PubMed: 19022501]
26. Allen LT, Tosetto M, Miller IS, O'Connor DP, Penney SC, Lynch I, Keenan AK, Pennington SR, Dawson KA, Gallagher WM. Surface-induced changes in protein adsorption and implications for

cellular phenotypic responses to surface interaction. Biomaterials. 2006; 27:3096–3108. [PubMed: 16460797]

27. Lynch I, Dawson KA. Protein-nanoparticle interactions. Nano Today. 2008; 3:40–47.
28. Flynn NT, Tran TNT, Cima MJ, Langer R. Long-term stability of self-assembled monolayers in biological media. Langmuir. 2003; 19:10909–10915.
29. Nelson CM, Raghavan S, Tan JL, Chen CS. Degradation of micropatterned surfaces by cell-Dependent and -independent processes. Langmuir. 2002; 19:1493–1499.
30. Ma H, Wells M, Beebe TP, Chilkoti A. Surface-initiated atom transfer radical polymerization of oligo(ethylene glycol) methyl methacrylate from a mixed self-assembled monolayer on gold. Adv Funct Mater. 2006; 16:640–648.
31. Mrksich M, Dike LE, Tien J, Ingber DE, Whitesides GM. Using microcontact printing to pattern the attachment of mammalian cells to self-assembled monolayers of alkanethiolates on transparent films of gold and silver. Exp Cell Res. 1997; 235:305–313. [PubMed: 9299154]
32. Capadona JR, Collard DM, García AJ. Fibronectin adsorption and cell adhesion to mixed monolayers of tri(ethylene glycol)- and methyl-terminated alkanethiols. Langmuir. 2002; 19:1847–1852.
33. Petrie TA, Capadona JR, Reyes CD, Garcia AJ. Integrin specificity and enhanced cellular activities associated with surfaces presenting a recombinant fibronectin fragment compared to RGD supports. Biomaterials. 2006; 27:5459–70. [PubMed: 16846640]
34. Abuchowski A, McCoy JR, Palczuk NC, van Es T, Davis FF. Effect of covalent attachment of polyethylene glycol on immunogenicity and circulating life of bovine liver catalase. J Biol Chem. 1977; 252:3582–6. [PubMed: 16907]
35. Raynor JE, Petrie TA, García AJ, Collard DM. Controlling cell adhesion to titanium: Functionalization of poly [oligo(ethylene glycol)methacrylate] brushes with cell-adhesive peptides. Adv Mater. 2007; 19:1724–1728.
36. Raynor JE, Capadona JR, Collard DM, Petrie TA, Garcia AJ. Polymer brushes and self-assembled monolayers: Versatile platforms to control cell adhesion to biomaterials (Review). Biointerphases. 2009; 4:FA3–16. [PubMed: 20408714]
37. Zammarelli N, Luksin M, Raschke H, Hergenröder R, Weberskirch R. “Grafting-from” polymerization of PMMA from stainless steel surfaces by a RAFT-mediated polymerization process. Langmuir. 2013; 29:12834–12843. [PubMed: 24053195]
38. Li B, Yu B, Ye Q, Zhou F. Tapping the potential of polymer brushes through synthesis. Acc Chem Res. 2015; 48:229–37. [PubMed: 25521476]
39. Jhon YK, Arifuzzaman S, Ozcam AE, Kiserow DJ, Genzer J. Formation of polyampholyte brushes via controlled radical polymerization and their assembly in solution. Langmuir. 2012; 28:872–82. [PubMed: 22112235]
40. Harder P, Grunze M, Dahint R, Whitesides GM, Laibinis PE. Molecular conformation in oligo(ethylene glycol)-terminated self-assembled monolayers on gold and silver surfaces determines their ability to resist protein adsorption. J Phys Chem B. 1998; 102:426–436.
41. Ostuni E, Chapman RG, Holmlin RE, Takayama S, Whitesides GM. A survey of structure–property relationships of surfaces that resist the adsorption of protein. Langmuir. 2001; 17:5605–5620.
42. Xiao Y, Zhao L, Shi Y, Liu N, Liu Y, Liu B, Xu Q, He C, Chen X. Surface modification of 316L stainless steel by grafting methoxy poly(ethylene glycol) to improve the biocompatibility. Chem Res Chin Univ. 2015; 31:1–7.
43. Lee H, Dellatore SM, Miller WM, Messersmith PB. Mussel-inspired surface chemistry for multifunctional coatings. Science. 2007; 318:426–30. [PubMed: 17947576]
44. Wang WC, Wang J, Liao Y, Zhang L, Cao B, Song G, She X. Surface initiated ATRP of acrylic acid on dopamine-functionalized AAO membranes. J Appl Polym Sci. 2010; 117:534–541.
45. Jin X, Yuan J, Shen J. Zwitterionic polymer brushes via dopamine-initiated ATRP from PET sheets for improving hemocompatible and antifouling properties. Colloids Surf B Biointerfaces. 2016; 145:275–84. [PubMed: 27208441]
46. Li CY, Wang WC, Xu FJ, Zhang LQ, Yang WT. Preparation of pH-sensitive membranes via dopamine-initiated atom transfer radical polymerization. J Membr Sci. 2011; 367:7–13.

47. Sin MC, Sun YM, Chang Y. Zwitterionic-based stainless steel with well-defined polysulfobetaine brushes for general bioadhesive control. ACS Appl Mater Interfaces. 2014; 6:861–73. [PubMed: 24351074]
48. Zangmeister RA, Morris TA, Tarlov MJ. Characterization of polydopamine thin films deposited at short times by autoxidation of dopamine. Langmuir. 2013; 29:8619–8628. [PubMed: 23750451]
49. Ma H, Li D, Sheng X, Zhao B, Chilkoti A. Protein-resistant polymer coatings on silicon oxide by surface-initiated atom transfer radical polymerization. Langmuir. 2006; 22:3751–3756. [PubMed: 16584252]
50. García AJ. Get a grip: integrins in cell–biomaterial interactions. Biomaterials. 2005; 26:7525–7529. [PubMed: 16002137]
51. Noga DE, Petrie TA, Kumar A, Weck M, García AJ, Collard DM. Synthesis and modification of functional poly(lactide) copolymers: Toward biofunctional materials. Biomacromolecules. 2008; 9:2056–2062. [PubMed: 18576683]
52. Liu X, Liu HB, Guo PF, Xiao SJ. Construction of multiple generation nitriloacetates from poly(PEGMA) brushes on planar silicon surface for enhancement of protein loading. Physica Status Solidi. 2011; 208:1462–1470.
53. Ren X, Wu Y, Cheng Y, Ma H, Wei S. Fibronectin and bone morphogenetic protein-2-decorated poly(OEGMA-r-HEMA) brushes promote osseointegration of titanium surfaces. Langmuir. 2011; 27:12069–73. [PubMed: 21888364]
54. Kumagai H, Tajima M, Ueno Y, Giga-Hama Y, Ohba M. Effect of cyclic RGD peptide on cell adhesion and tumor metastasis. Biochem Biophys Res Commun. 1991; 177:74–82. [PubMed: 1710455]
55. Lutolf MP, Weber FE, Schmoekel HG, Schense JC, Kohler T, Muller R, Hubbell JA. Repair of bone defects using synthetic mimetics of collagenous extracellular matrices. Nat Biotechnol. 2003; 21:513–8. [PubMed: 12704396]
56. Lutolf MP, Hubbell JA. Synthetic biomaterials as instructive extracellular microenvironments for morphogenesis in tissue engineering. Nat Biotechnol. 2005; 23:47–55. [PubMed: 15637621]
57. Petrie TA, Raynor JE, Dumbauld DW, Lee TT, Jagtap S, Templeman KL, Collard DM, Garcia AJ. Multivalent integrin-specific ligands enhance tissue healing and biomaterial integration. Sci Transl Med. 2010; 2:45ra60.
58. Wang JS, Matyjaszewski K. Controlled/”living” radical polymerization. atom transfer radical polymerization in the presence of transition-metal complexes. J Am Chem Soc. 1995; 117:5614–5615.
59. Jin Z, Brash JL, Zhu S. ATRP grafting of oligo(ethylene glycol) methacrylates from gold surface — Effect of monomer size on grafted chain and EO unit densities. Can J Chem. 2010; 88:411–417.
60. Feng W, Nieh MP, Zhu S, Harroun TA, Katsaras J, Brash JL. Characterization of protein resistant, grafted methacrylate polymer layers bearing oligo(ethylene glycol) and phosphorylcholine side chains by neutron reflectometry. Biointerphases. 2007; 2:34–43. [PubMed: 20408634]
61. Ohno K, Tabata H, Tsujii Y. Surface-initiated living radical polymerization from silica particles functionalized with poly(ethylene glycol)-carrying initiator. Colloid Polym Sci. 2013; 291:127–135.

Statement of Significance

Stainless steel (SS) implants are widely used clinically for orthopaedic, spinal, dental and cardiovascular applications. However, non-specific adsorption of biomolecules onto implant surfaces results in sub-optimal integration with host tissue. To allow controlled cell-SS interactions, we have developed a strategy to grow non-fouling polymer brushes that prevent protein adsorption and cell adhesion and can be subsequently functionalized with adhesive peptides to direct cell adhesion and signaling. This approach has broad application to improve osseointegration onto stainless steel implants in bone repair.

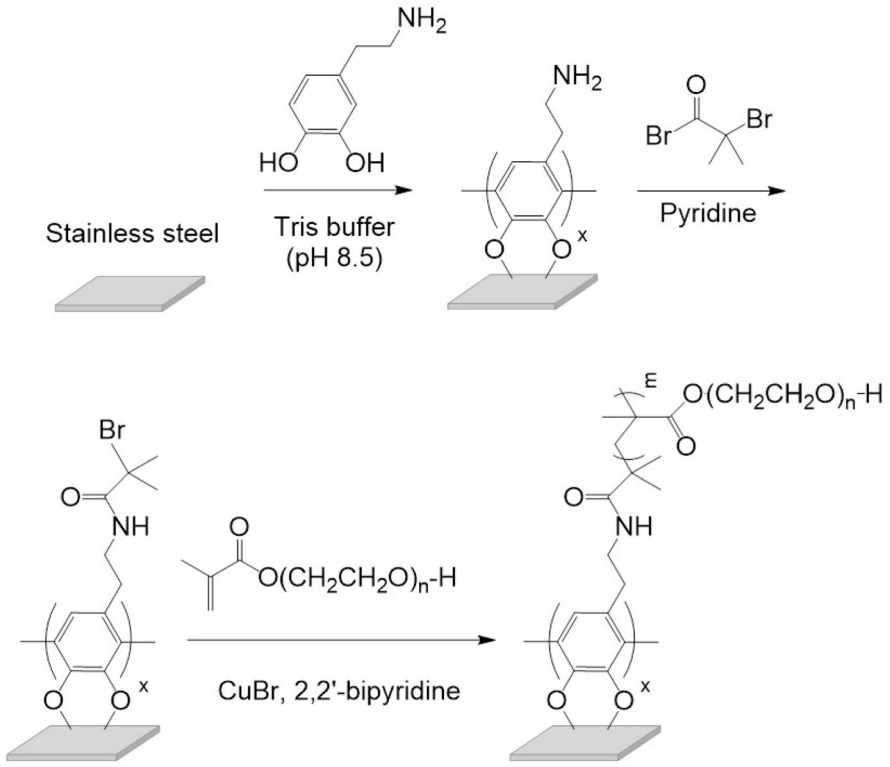

Figure 1.
Scheme for the formation of poly(OEGMA) brushes on SS.

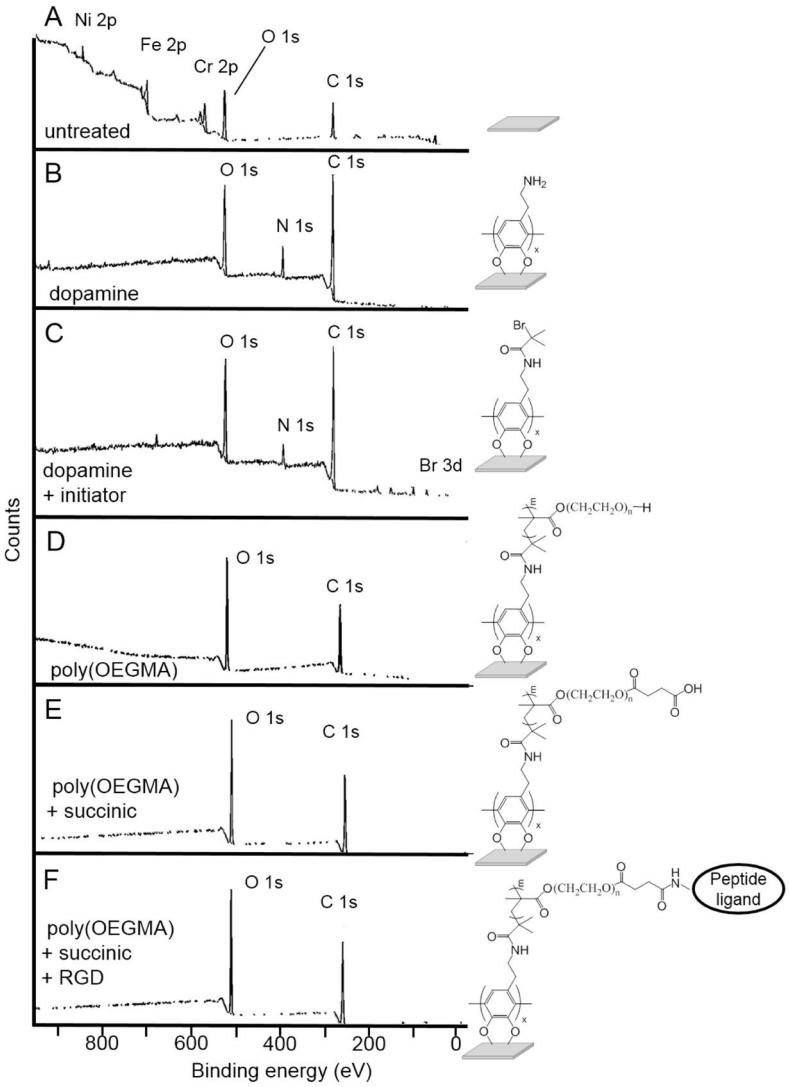

Figure 2.

XPS survey spectra of untreated and poly(OEGMA) brush-modified SS: (A) untreated SS surfaces, (B) polydopamine SS surfaces, (C) attached initiator polydopamine SS surface, (D) poly(OEGMA) SS, (E) poly(OEGMA) with tethered succinic acid, and (F) poly(OEGMA) with tethered ligand.

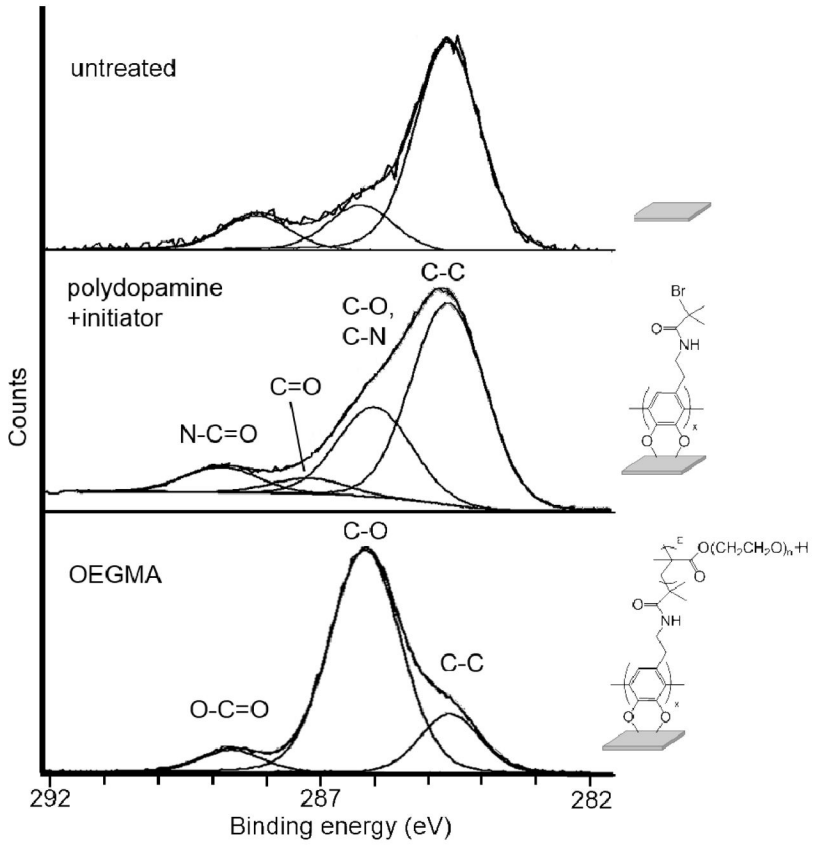

Figure 3.

High resolution XPS scan of the carbon 1*s* region of the spectrum of SS coupons: Untreated SS (top), polydopamine + initiator (middle), and poly(OEGMA)-modified SS (bottom) (C=O in spectrum of polydopamine + initiator results from the oxidation of catechol unit [48]).

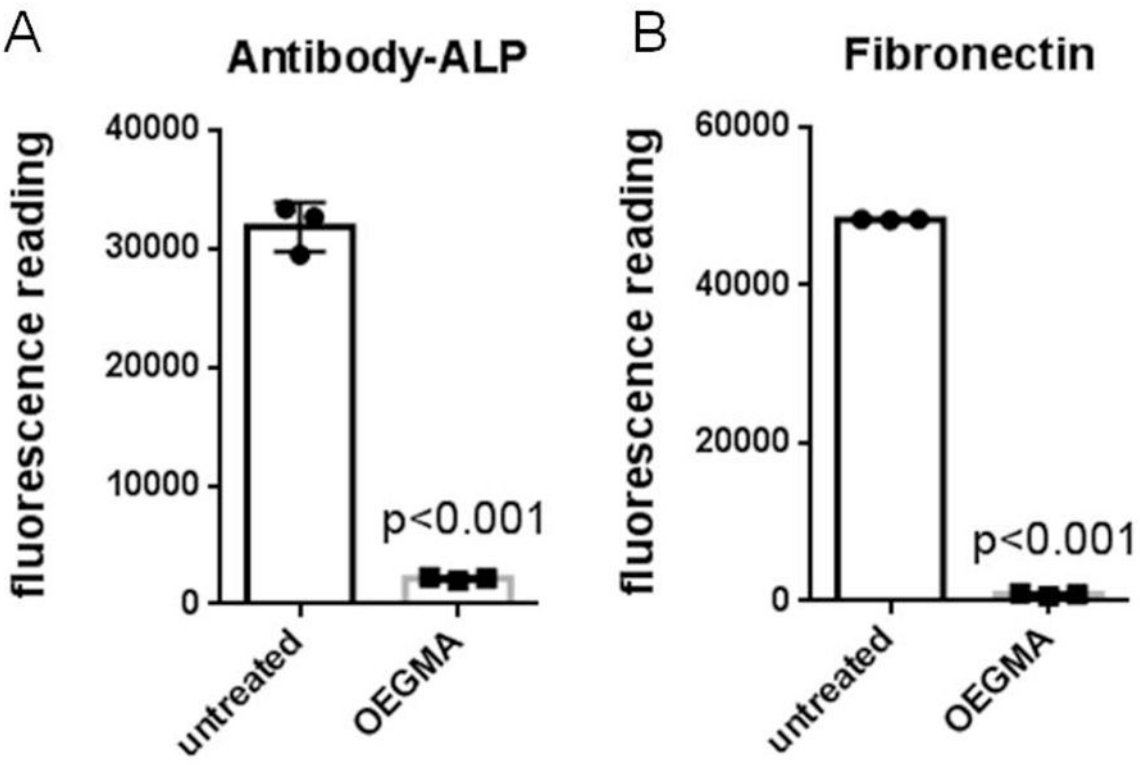

Figure 4.

poly(OEGMA) brush results in reduced protein adsorption on SS surface. Protein adsorption on untreated and poly(OEGMA) coupons: (A) alkaline phosphatase-conjugated antibody, and (B) human fibronectin.

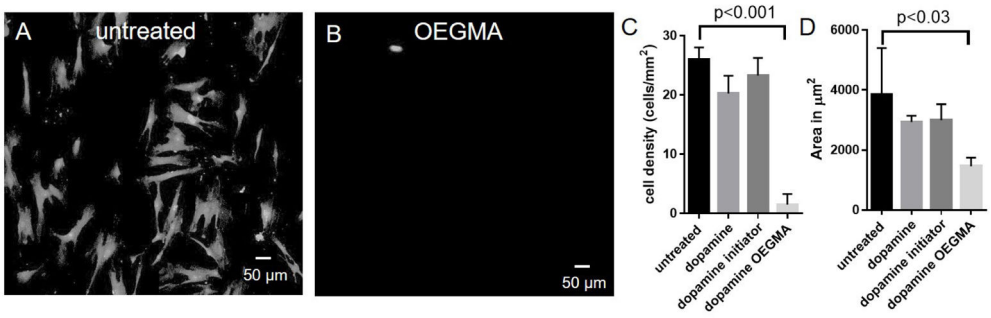

Figure 5.

poly(OEGMA) brush prevents cell attachment on SS surface. Fluorescent microscope images of human mesenchymal stem cells (hMSCs) stained with Calcein-AM: (A) untreated SS surfaces, and (B) poly(OEGMA) SS surfaces. Quantification of hMSC density and spreading on untreated and poly(OEGMA) brushes: (C) adherent cell density, and (D) cell spreading area.

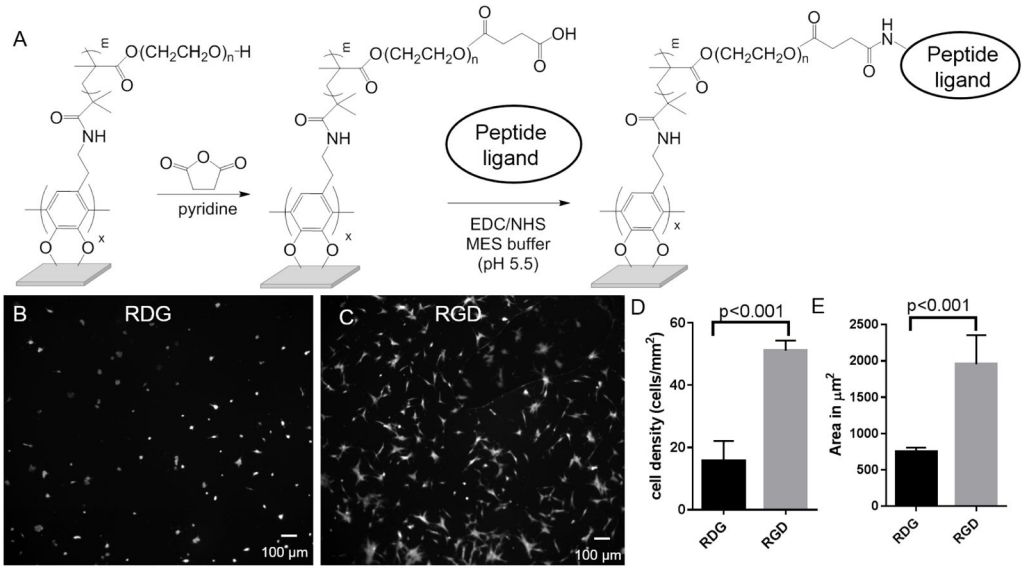

Figure 6.

Peptide functionalized poly(OEGMA) brushes result in controlled cell attachment to SS surface. (A) Scheme for modification of poly(OEGMA) brushes with peptides. Fluorescent microscope images of hMSCs stained with Calcein-AM on peptide modified poly(OEGMA) brushes: (B) RDG modified surfaces, and (C) RGD treated brushes. Quantification of (D) adherent cell density, and (E) cell spreading area for hMSCs on RDG- and RGD-modified poly(OEGMA) brushes.

Table 1

Water contact angle measurements for SS coupons.

Treatment	water contact angle
clean SS	6 ± 3°
polydopamine	31 ± 3°
initiator attachment	77 ± 5°
poly(OEGMA) growth	52 ± 4°

Table 2

XPS non-metal surface composition of SS modification (%)

	C	O	N	Br
untreated	26.9	50.7	0	0
polydopamine	71.4	20.5	7.7	0
initiator attachment	69.8	20.6	4.5	2.2
poly(OEGMA)	65.5	32.4	0	0
succinc acid modification	67.4	31.6	0	0
peptide tethering	66.7	31.3	0	0

Table 3

XPS C1*s* analysis of initiator attachment and poly(OEGMA) SS (%)

	C-C	C-O	O-C=O	C=O	C-O, C-N	N-C=O
initiator attachment	60.8	0	0	4.70	27.0	7.60
poly(OEGMA)	17.4	76.3	6.30	0	0	0